Journal of Applied Polymer Science

Synthesis and characterization of polyimide/modified mCOC composites

Yao-Yi Cheng,[1] Hsin-Min Hsiao,[1] Zong-Xuan Li,[1] Ming-Jaan Ho,[2] Mao-Feng Hsu,[2] Shou-Jui Hsiang[2]

[1]Institute of Organic and Polymeric Materials, National Taipei University of Technology, 1, Sec. 3, Chung-hsiao E. Road, Taipei, Taiwan 10608, Republic of China

[2]Zhen Ding Technology Holding Limited, No. 6, Lane 28, Sanhe Road, Sanshi Village, Dayuan, Taoyuan, Taiwan 33754, Republic of China

Correspondence to: Y.-Y. Cheng (E-mail: ycheng@mail.ntut.edu.tw)

ABSTRACT: Two types of monomers, 4,4′-(hexafluoroisopropylidene) diphthalic anhydride and 4,4′-oxydianiline, were employed to synthesize poly(amic acid) (PAA) as a precursor of polyimide (PI). Through the addition of modified metallocene cyclic olefin copolymer (mCOC), PAA/mCOC composites were formed. PI/mCOC composites were obtained through a blade coating and multistep thermal curing process. The structure of the prepared PI/mCOC composites was characterized through Fourier transform infrared spectrometry. The results showed that the copolymerization of PAA and modified mCOC improved thethermal stability and hydrophobic and electrical properties of the PI/mCOC composites. The formation of a network structure between PI and modified mCOC considerably reduced the mobility of PI molecules, thereby improving the glass transition temperature and thermal properties of the composite. The thermal and hydrophobic properties were improved by increasing the mCOC grafting ratio. © 2016 Wiley Periodicals, Inc. J. Appl. Polym. Sci. **2016**, *133*, 44144.

KEYWORDS: composites; grafting; polyimides

Received 12 April 2016; accepted 25 June 2016
DOI: 10.1002/app.44144

INTRODUCTION

In recent years, flexible printed circuit boards (FPCBs) have proved advantageous to realizing a light module with a small volume. Because of its thinness, high thermal resistance, and superior flexibility, an FPCB can be attached to an arbitrary curved surface.[1] Many types of substrates have been used for FPCBs, such as polymer, textile, and silicon. Over the past few years, polymeric materials, such as polyimide (PI), have been used to manufacture FPCBs and membrane switches.[2]

PI is one of the most promising high-performance polymers possessing high thermal stability, excellent mechanical and electrical insulation properties, and chemical stability.[3] Therefore, PI can be used in optoelectronics, electronics, adhesives, and aerospace applications. The polymerization of PI is a two-step procedure that has been used to manufacture nanocomposites.[4] First, the reaction of an aromatic diamine with an aromatic dianhydride[5] is conducted in polar aprotic solvents to form a precursor solution, poly(amic acid) (PAA). A chemical method or multistep thermal curing is then used for fabricating PI films.[6,7]

Metallocene cyclic olefin copolymer (mCOC), which has a high glass transition temperature (T_g) and excellent mechanical, dielectric, and optical properties, can be used as a heat-resistant, dielectric material and in optical applications.[8–13] In this study, we incorporated mCOC into a PI matrix. However, the lack of a chemically bonded moiety between mCOC and the PI matrix results in phase separation and facile aggregation. To enhance dispersion within a PI matrix, modifying mCOC with functional groups is necessary. Through solution grafting modification, maleic anhydride (MA) was grafted onto the olefin backbone of mCOC. PI/modified mCOC composites were prepared by polymerizing PI from PAA loaded with modified mCOC. Their thermal, hydrophobic, and electrical properties were studied.

EXPERIMENTAL

Materials

mCOC (TOPAS-6015), MA (Alfa Aesar, 98%), cis-5-norbornene-endo-2, benzoyl peroxide (BOP, Alfa Aesar, 97%), 4,4′-(hexafluoroisopropylidene) diphthalic anhydride (6FDA, Chriskev, 98%), 4,4′-oxydianiline (ODA, Chriskev, 99%), potassium hydrogen phthalate (Sigma-Aldrich, 99.95%), potassium hydroxide (KOH, SHOWA, 85%), toluene (ECHO CHEMICAL, 99%), methanol (Echo Chemical, 99%), and 1-methyl-2-pyrrolodinone (NMP, Acros, 99%) were used as received without further purification.

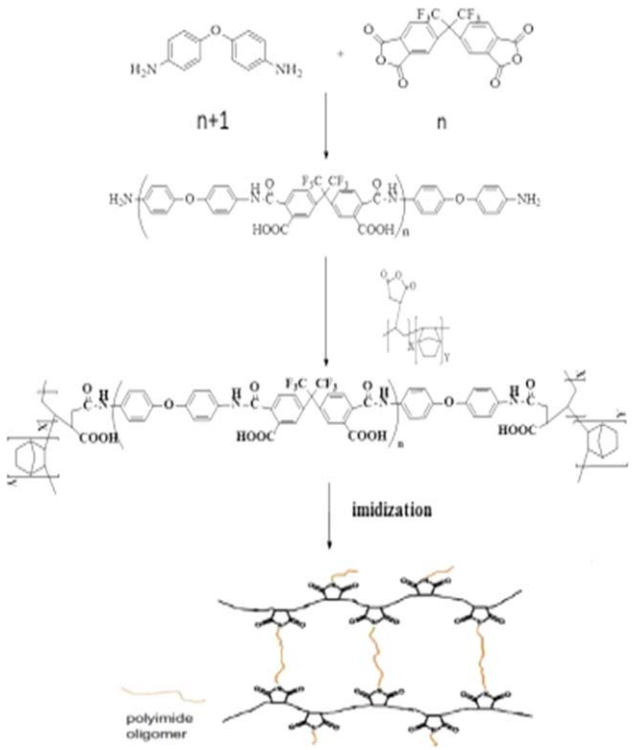

Figure 1. Reaction scheme for preparing PI/mCOC-MA composites. [Color figure can be viewed in the online issue, which is available at wileyonlinelibrary.com.]

Preparation of mCOC-MA

mCOC was added to a flask and dissolved in toluene. MA and BOP were added and reacted at 120 °C under nitrogen for 6 h; subsequently, methanol was added to the flask to stop the reaction. The precipitate was washed three times with DI water and then vacuum dried at 120 °C for 2 h.

Preparation of PAA

For preparing PI precursors, PAA, diamine ODA (1.87 mmol) was added to a flask and dissolved in NMP (8.7 g) with vigorous stirring. After 30 min, the dianhydride 6FDA (1.82 mmol) was added and reacted at room temperature in an atmospheric environment for 24 h. The PAA solution was obtained with 12 wt % solid content. To control the molecular weight, the molar ratio of ODA to 6FDA was kept as 1.03:1.[14–19]

Preparation of PAA/mCOC-MA Composites by Blending

mCOC-MA was added to a flask and dissolved in toluene with stirring. The resulting solution was slowly added to the PAA solution. The mixture was stirred at room temperature in an atmospheric environment for 24 h to obtain PAA/mCOC-MA composites. Figure 1 shows the reaction scheme.

Synthesis of PI/mCOC Hybrid Films

PI/mCOC films were prepared by coating glass plates with the PAA solution and subjecting them to multistep thermal curing at 100, 150, 200, and 250 °C for 1 h and then at 300 °C for 2 h.

Characterization

FT-IR analysis was performed using a Perkin-Elmer RXI-FT-IR system. To determine the acid content of modified mCOC,

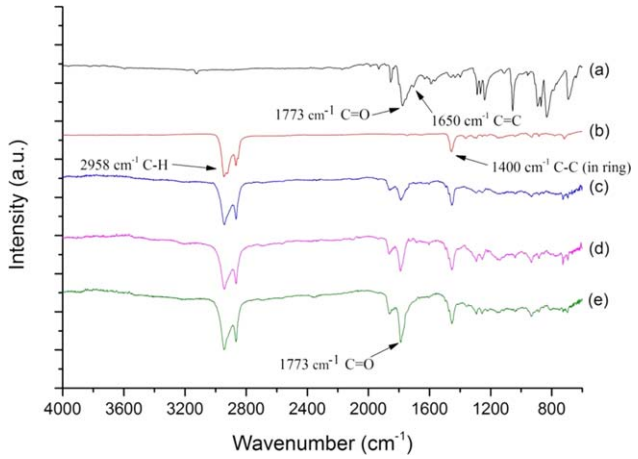

Figure 2. FT-IR spectra: (a) MA, (b) mCOC, (c) mCOC-MA1, (d) mCOC-MA2, and (e) mCOC-MA3. [Color figure can be viewed in the online issue, which is available at wileyonlinelibrary.com.]

0.1 g of mCOC-MA or mCOC-NA was added to 20 mL of toluene, stirred at 120 °C for 2 h, and then neutralized by titrating a 0.01*N* KOH solution. Thermal gravimetric analysis (TGA) was performed using a TA (Seilp SSC 5000, Japan) in nitrogen from 35 to 900 °C at a heating rate of 10 °C/min. Dynamic mechanical measurements were conducted on a Perkin-Elmer DMA7e. Temperature scans were performed from +30 to +320 °C under heating rate of 5 °C/min. The scanning frequency was 1 Hz. A contact angle test was performed using a Phoenix-300 Touch system. Water absorbency was examined using IPC-TM-650 Test Methods. Electrical properties were measured using an ULTRA Mosoh-meter SM-8200, and a test was conducted at room temperature and a constant voltage of 1000 V.

RESULTS AND DISCUSSION

Figure 2 shows a comparison of the FT-IR spectra of MA, mCOC, and mCOC-MA. In traces (b), (c), (d), and (e), the characteristic absorption bands of mCOC can be observed at 2958 and 1400 cm^{-1} for the C—H and C—C groups, respectively. In trace (a), the characteristic absorption bands of MA can be observed at 1773 and 1650 cm^{-1} for the C=O and C=C groups, respectively. In traces (c), (d), and (e), the grafting of MA to mCOC is evidenced by the disappearance of C=C

Table I. Grafting Ratio of mCOC-MA

Sample	mCOC (mol)	BO (mol)	MA (mol)	Grafting ratio (wt %)
	100	2.5	12.5	0.62
MA1	100	2.5	25	1.12
	100	2.5	50	1.83
	100	2.5	100	2.76
	100	2.5	50	1.83
	100	5	50	2.24
MA3	100	10	50	3.10
MA2	100	20	50	2.01

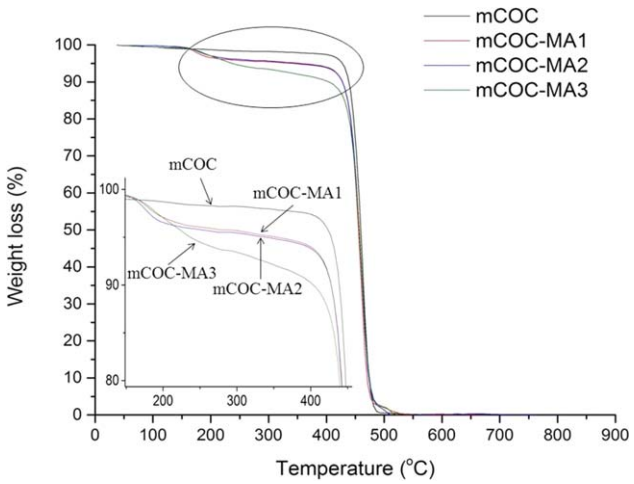

Figure 3. TGA profiles of difference grafting ratio of mCOC, mCOC-MA1, mCOC-MA2, and mCOC-MA3 under nitrogen atmosphere. [Color figure can be viewed in the online issue, which is available at wileyonlinelibrary.com.]

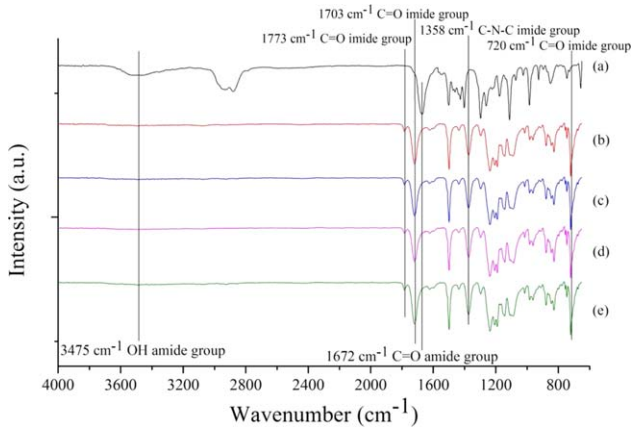

Figure 4. FT-IR spectra: (a) PAA, (b) PI, (c) PI/mCOC-MA1, (d) PI/mCOC-MA2, and (e) PI/mCOC-MA3 composites. [Color figure can be viewed in the online issue, which is available at wileyonlinelibrary.com.]

absorption at 1650 cm^{-1} and the increase of C═O adsorption at 1773 cm^{-1}.

Table I shows the grafting ratios for mCOC-MA determined through titration. These results demonstrated that the grafting ratio increased as more MA was added to react with mCOC. mCOC-MA with a grafting ratio of 1.12% was designated MA1. The grafting ratio increased gradually as the amount of initiator BOP increased. When the concentration ratio of mCOC to BOP was 10:1, the grafting ratio was the highest. The excess free radicals produced with a further increase in the ratio of mCOC to BOP to 5:1 reduced the mCOC-MA grafting ratio to 2.01%; the sample with this grafting ratio was designated MA2. The mCOC-MA with the highest grafting ratio of 3.10% was designated MA3.

Figure 3 illustrates TGA curves of mCOC and its grafts, and Table II summarizes the results. The decomposition temperature at 10% weight loss, T_{10} (°C), and maximum decomposition rate, T_d, of pure mCOC were 439 and 462 °C, respectively, and mCOC-MA exhibited reduced thermostability. The decomposition temperature at 5% weight loss T_5 (°C) and T_{10} (°C) of mCOC-MA composites decreased as the MA grafting amount increased; MA decomposed at a low temperature. Nevertheless, the maximum decomposition rate of mCOC-MA was almost unaffected by MA grafting.

A two-step procedure is commonly used for preparing PI films. First, through the ring opening polyaddition of aromatic dianhydride and diamine to a polar aprotic NMP solution, a PAA solution in which modified mCOC can be stably dispersed is formed. Through thermal curing, PAA/mCOC composites can then be converted to PI/mCOC networks, as shown in Figure 1. Figure 4 provides a comparison of the FT-IR spectra of PAA, PI and PI/modified mCOC composites. The conversion of PAA to PI can be explained by the characteristic absorption bands of the amide group observed at 3475 (carbonyl acid O-H), 1672 (C═ONH stretching vibration) and 1537cm^{-1} (CNH vibration) disappeared, while the imide group observed at 1773 (C═O asymmetric stretching), 1703 (C═O symmetric stretching), 1358 cm^{-1} (C—N—C imide ring stretching) and 720 (C═O symmetric stretching) newly appeared.

Table II. Thermal Properties of mCOC, mCOC Grafts, PI, and PI/mCOC-MA Composites

Sample	T_g (°C)[a]	T_5 (°C)[b]	T_{10} (°C)[c]	T_d (°C)[d]	R_c (%)[e]
mCOC	—	428	439	462	0
mCOC-MA1	—	346	431	462	0
mCOC-MA2	—	344	429	461	0
mCOC-MA3	—	237	404	461	0
PI	300	439	511	545	45
PI/mCOC-MA1	306	443.	515	546	47
PI/mCOC-MA2	306	486	521	546	49
PI/mCOC-MA3	309	493	523	547	49

[a] T_g, glass transition temperature.
[b] T_5, 5% decomposition temperature.
[c] T_{10}, 10% decomposition temperature.
[d] T_d, decomposition temperature at the maximum decomposition rate.
[e] Residues of TGA analysis at 900 °C.

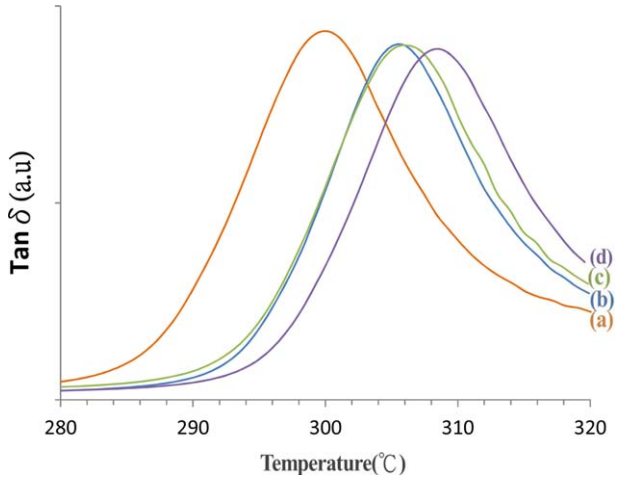

Figure 5. Tan δ of DMA of (a) PI, (b) PI/mCOC-MA1, (c) PI/mCOC-MA2, and (d) PI/mCOC-MA3 composites. [Color figure can be viewed in the online issue, which is available at wileyonlinelibrary.com.]

Figure 5 shows tan δ (glass-transition region) for PI and PI/mCOC-MA composites, and Table II summarizes the results. The T_g of the PI/mCOC composites was higher than that of pure PI. The T_g increased considerably with an increase in the grafting ratio of mCOC-MA because when PAA was added to the mCOC-MA, the amine group of PAA reacted with the anhydride group of mCOC-MA to form an imide group, and a network structure was thus produced (Figure 1). The higher the mCOC-MA grafting ratio is, the more cross-links the network has. When the mCOC-MA grafting ratio reached 3%, the maximum T_g of the PI/mCOC-MA composites was 309 °C.

Figure 6 illustrates the TGA curves of PI and PI/mCOC-MA composites, and Table II summarizes the results. The T_5 (°C) and T_{10} (°C) of PI were 439 and 511 °C, respectively, and the PI/mCOC-MA composites demonstrated enhanced thermo stability. As the cross-linking of the PI/mCOC-MA composites

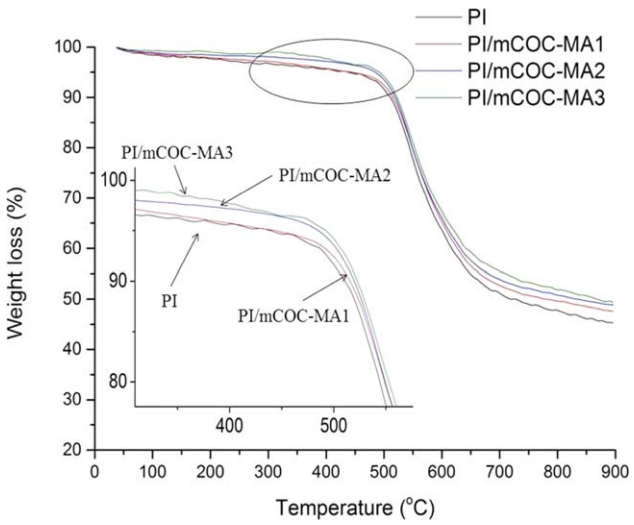

Figure 6. TGA profiles of (a) PI, (b) PI/mCOC-MA1, (c) PI/mCOC-MA2, and (d) PI/mCOC-MA3 under nitrogen atmosphere. [Color figure can be viewed in the online issue, which is available at wileyonlinelibrary.com.]

Table III. Contact Angle of mCOC, mCOC-MA Grafts, PI, and PI/mCOC-MA Composites

Grafting ratio (wt %)	mCOC (°)	mCOC-MA (°)	PI (°)	PI/mCOC-MA (°)
0	89.9	—	77.0	—
1	—	85.3	—	94.0
2	—	81.6	—	96.0
3	—	72.0	—	101.9

increased with an increase in the mCOC-MA grafting ratio, the T_5 (°C) and T_{10} (°C) of the PI/mCOC-MA composites considerably increased, which suggesting that a perfect network structure could be formed. For PI/mCOC-MA3, T_5 (°C) and T_{10} (°C) reached maximal values of 493 and 523 °C, respectively.

Table III shows the contact angles of mCOC, mCOC grafts, PI, and PI/mCOC composites. These results demonstrated that when mCOC was grafted with MA, the contact angle decreased. Because the anhydride group of MA is hydrophilic, the contact angle of mCOC-MA decreased as the MA grafting ratio increased. However, the contact angle of PI/mCOC-MA composites was higher than that of pure hydrophobic PI. As the mCOC-MA grafting ratio increased, the contact angle of the PI/mCOC-MA composites increased, proving that PI and mCOC-MA formed a perfect network structure.

Water absorbance was measured to study the hygroscopic property of the PI/mCOC composites by soaking the PI/mCOC-MA composite film in deionized water for 24 h. Table IV shows the hygroscopic properties of PI and the PI/mCOC-MA composites. The water absorbance of the PI/mCOC-MA composites was lower than that of pure PI. As the mCOC-MA grafting ratio increased, PI could form a network with more mCOC, thereby increasing its hydrophobicity. The lowest water absorbance was 1.62% at the grafting ratio of 3% for the PI/mCOC-MA composites.

Table V shows the electrical properties of PI and PI/mCOC-MA composites at various grafting ratios. Pure PI is an insulator with a surface resistance of 3.74×10^{14} Ω/cm^2. The surface resistance of the PI composites increased as the mCOC-MA grafting ratio increased. Table V shows that the surface resistance of PI/mCOC-MA composites can be improved by at least four times relative to that of pure PI. The surface resistance increased because mCOC imparted an excellent electrical insulating property. The highest surface resistance achieved was 9.31×10^{15}Ω/cm^2 when the mCOC-MA grafting ratio was 3%.

Table IV. Hygroscopic Properties of PI and PI/mCOC-MA Composites

Grafting ratio (wt %)	PI (wt %)	PI/mCOC-MA (wt %)
0	1.93	—
1	—	1.82
2	—	1.73
3	—	1.62

Table V. Surface Resistance of PI and PI/mCOC-MA Composites

Grafting ratio (wt %)	PI (Ω/cm^2)	PI/mCOC-MA (Ω/cm^2)
0	3.74×10^{14}	—
1	—	1.67×10^{15}
2	—	6.92×10^{15}
3	—	9.31×10^{15}

CONCLUSIONS

PI/modified mCOC composites were successfully fabricated. mCOC was grafted with MA to enhance its dispersion within the PI matrix. When the amine groups of PAA reacted with the anhydride groups of mCOC-MA, a network structure was produced. Consequently, the thermal properties of PI/mCOC-MA composites were superior to those of pure PI. When the mCOC-MA grafting ratio was increased, both the T_g and the decomposition temperature of the PI/mCOC-MA composites increased. The T_g and T_{10} (°C) of PI were 300 and 511 °C, respectively. As the mCOC-MA grafting ratio reached 3%, the T_g and T_{10} (°C) of the PI/mCOC-MA composites reached maximal values of 309 and 523 °C, respectively. Furthermore, as the mCOC-MA grafting ratio increased, the hydrophobic property and surface resistivity of the PI/mCOC-MA composites increased, thus proving that the PI/mCOC-MA composites formed a perfect network structure.

ACKNOWLEDGMENTS

We thank the financial support from Zhen Ding Technology Holding Limited. The financial support and information consultancy of hign end flexible material development trends provided by Zhen Ding Technology Limited is greatly appreciated

REFERENCES

1. Teng, M. F.; Hariz, A.; Hsu, H. Y.; Omari, T. *Microelectronics* **2007**, *6798*, D7981.
2. Kim, B. S.; Bae, S. H.; Park, Y. H.; Kim, J. H. *Int. Conf. Nanosci. Nanotechnol.* **2006**, *1*, 26.
3. Tang, Q. Y.; Chan, C. N.; Wong, B.; Cheung, R. *Polym. Int.* **2010**, *59*, 1240.
4. Haggenmueller, R.; Du, F.; Fischer, J. E.; Winey, K. I. *Polymer* **2006**, *47*, 2381.
5. Chen, T. A.; Jen, A. K. Y.; Cai, Y. *J. Am. Chem. Soc.* **1995**, *117*, 7295.
6. Hergenrother, P. M.; Watson, K. A.; Smith, J. G. Jr.; Connell, J. W.; Yokota, R. *Polymer* **2002**, *43*, 5077.
7. Ko, H. H.; Cheng, Y. Y.; Wang, C. W. *Nanosci. Nanotechnol.* **2013**, *5*, 1.
8. Yamazaki, M. *J. Mol. Catal. A* **2004**, *213*, 81.
9. Mase, H.; Kondo, M.; Matsuda, A. *Sol. Energy Mater. Sol. Cells* **2002**, *74*, 547.
10. Forsyth, J.; Perena, J. M.; Benavente, R.; Perez, E.; Tritto, I.; Boggioni, L.; Brintzinger, H. H. *Macromol. Chem. Phys.* **2001**, *2*, 202.
11. Harrington, B. A.; Crowther, D. J. *J. Mol. Catal. A* **1998**, *128*, 79.
12. Wang, Q.; Weng, J.; Fan, Z.; Feng, L. *Macromol. Rapid Commum.* **1997**, *18*, 1101.
13. Bergström, C. H.; Väänänen, T. L. J.; Seppälä, J. V. *J. Appl. Polym. Sci.* **1997**, *63*, 1071.
14. Meador, M. A. B.; Aleman, C. R.; Hanson, K.; Ramirez, N.; Vivod, S. L.; Wilmoth, N.; McCorkle, L. *Appl. Mater.* **2015**, *7*, 1240.
15. Williams, J. C.; Meador, M. A. B.; Mc Corkle, L.; Mueller, C.; Wilmoth, N. *Chem. Mater.* **2014**, *26*, 4163.
16. Meador, M. A. B.; McMillon, E.; Sandberg, A.; Barrios, E.; Wilmoth, N.; Mueller, C. H.; Miranda, F. A. *Appl. Mater.* **2014**, *6*, 6062.
17. Meador, M. A. B.; Malow, E. J.; Silva, R.; Wright, S.; Quade, D.; Vivod, S. L.; Guo, H. Q.; Guo, J.; Cakmak, M. *Appl. Mater.* **2012**, *4*, 536.
18. Meador, M. A. B.; Wright, S.; Sandberg, A.; Nguyen, B. N.; Van Keuls, F. W.; Mueller, C. H.; Rodriguez-Solis, R.; Miranda, F. A. *Appl. Mater.* **2012**, *4*, 6346.
19. Du, A.; Zhou, B.; Zhang, Z.; Shen, J. *Materials* **2013**, *6*, 941.